Endocrine (2016) 53:145–156
DOI 10.1007/s12020-015-0739-y

ORIGINAL ARTICLE

Molecular profiles of cancer stem-like cell populations in aggressive thyroid cancers

Mariavittoria Dima[1] · Valeria Pecce[1] · Mauro Biffoni[2] · Cira Rosaria Tiziana Di Gioia[3] · Giovanni Tallini[4] · Marco Biffoni[5] · Francesca Rosignolo[1] · Antonella Verrienti[1] · Marialuisa Sponziello[1] · Giuseppe Damante[6] · Diego Russo[7] · Cosimo Durante[1]

Received: 19 June 2015 / Accepted: 6 September 2015 / Published online: 14 September 2015

Abstract A substantial proportion of patients with advanced thyroid carcinoma fail to respond to or at some point become refractory to conventional therapies. This resistance and the phenomena of thyroid cancer progression and metastasis themselves are thought to be related to tumor-cell sub-populations with stem-like properties. We isolated thyrospheres from four advanced thyroid carcinomas that were resistant to radioiodine therapy and analyzed their molecular profiles. ALDH activity and proteomic profile of main stem cell markers were used to assess stem cell properties. The TaqMan Low Density Array approach was used to evaluate the expression of several genes involved in the EMT process. The phosphorylation status of tyrosine kinase receptors (RTKs) was analyzed to identify potential markers for targeted therapies. We then investigated the effects of the EMT-inhibitor crizotinib on both cell proliferation and phosphorylation status of RTK targets. The cancer stem-like properties of a subset of cells from primary cultures of each tumor were demonstrated. A wide variability among thyrospheres arising from the four thyroid cancers in terms of ALDH activity, stem cell marker expression, and phosphoproteome profiling was present. Dysregulated expression of genes involved in the EMT was observed in all four thyrosphere lines. Treatment with crizotinib was ineffective in cancer stem-like cells, suggesting the presence of a mechanism of resistance in thyrospheres. Collectively, our data indicate that thyroid cancer stem-like populations vary markedly from tumor to tumor and require detailed molecular and biological characterization if they are to be used as the basis of "personalized" treatment of aggressive disease.

Keywords Metastatic thyroid cancer · Epithelial-mesenchymal transition · Cancer stem cells · Drug resistance

Mariavittoria Dima and Valeria Pecce have contributed equally to this work.

Electronic supplementary material The online version of this article (doi:10.1007/s12020-015-0739-y) contains supplementary material, which is available to authorized users.

✉ Diego Russo
d.russo@unicz.it

1 Dipartimento di Medicina Interna e Specialità Mediche, Università di Roma "Sapienza", Rome, Italy

2 Dipartimento di Ematologia, Oncologia e Medicina Molecolare, Istituto Superiore di Sanità, Rome, Italy

3 Dipartimento di Scienze Radiologiche, Oncologiche ed Anatomopatologiche, Università di Roma "Sapienza", Rome, Italy

4 Dipartimento di Medicina Specialistica, Diagnostica e Sperimentale, Università di Bologna, Bologna, Italy

5 Dipartimento di Scienze Chirurgiche, Università di Roma "Sapienza", Rome, Italy

6 Dipartimento di Scienze Mediche e Biologiche, Università di Udine, Udine, Italy

7 Dipartimento di Scienze della Salute, Università di Catanzaro "Magna Graecia", Viale Europa, 88100 Catanzaro, Italy

Introduction

Radioactive iodine ablation (^{131}I administration) is currently the only effective treatment available for recurrent or metastatic papillary or follicular thyroid cancers. However, in two out of three patients with this type of disease, the tumors are characterized by defective uptake/concentration and/or decreased sensitivity to ^{131}I [1, 2] caused in most cases by the loss of functional sodium/iodide symporter

(NIS) expression [3–7]. Current evidence suggests that the spread of neoplastic disease and its resistance to conventional therapies are largely mediated by the so-called cancer stem cells [8], a relatively small subpopulation of tumor cells with the capacity for self-renewal [9]. Cancer stem-like cells (CSCs) have been identified in thyroid cancer tissues and continuous cell lines, and their stem-like properties appear to be closely related to the epithelial-mesenchymal transition (EMT), a process that is also involved in the physiological remodeling of tissues and cells during embryogenesis [10–13]. The EMT is characterized by repressed expression of E-cadherin and other adhesion molecules and the acquisition of mesenchymal features, which allow the cell to migrate to distant sites [14]. Indeed, in a study of human breast epithelial cells, the acquisition of mesenchymal traits was associated with the expression of known stem cell markers, and transformed cells that had undergone EMT displayed increased efficiency in the formation of spheres, soft agar colonies, and tumors. These findings imply that, in addition to enabling cancer cells to spread, the EMT program also sustains their capacity for self-renewal [15]. Characterization of CSCs from particularly aggressive thyroid cancers might thus reveal potentially useful information for novel, targeted treatments for these tumors.

In the present study, we explored the molecular profiles of thyrospheres derived from four metastatic thyroid cancers characterized by resistance to radioiodine therapy. Particular attention was focused on their expression of EMT-related genes, the activation status of EMT-related tyrosine kinase receptors (RTKs), and their responses to the broad-spectrum RTK inhibitor crizotinib.

Materials and methods

The study protocol was approved by the local ethics committee, and written informed consent was obtained from each patient whose tissues were used. Unless otherwise stated, all commercial products mentioned below were used according to the manufacturer's instructions and/or protocols.

Thyroid tissue collection

Tumor tissue samples were collected from four patients who consecutively underwent surgery in our hospital for primary, locally recurrent, and/or metastatic thyroid cancer, which had displayed resistance to radioiodine-based therapy. All tissue specimens were submitted for standard histopathological examination by two different pathologists, who confirmed the neoplastic phenotype. Clinical data on each case were collected from hospital charts, and tumors were staged according to the criteria of American Joint Committee on Cancer [16]. Molecular characterization of all tissue specimens was performed by Sanger Sequencing analysis of hot spots in thyroid cancer driver genes [i.e., *BRAF* (exon 15); *HRAS* (exon 2,3); *KRAS* (exon 2,3); *NRAS* (exon 2,3); *TP53* (exons 5–9); *PTEN* (exons 5–8)]. Details on mutation analysis have been provided elsewhere [17, 18]. For primers contact the authors.

Primary cell cultures and thyrosphere generation

After meticulous removal of fibrous tissues, the surgical specimens were minced with sterile scissors and incubated for 1 h at 37 °C in digestion medium consisting of DMEM/F12 1:1 and collagenase IV (1 mg/ml) (Gibco-BRL Division, Life Technologies, Foster City, CA). The resulting cell suspension was plated onto DMEM/F12 medium (Gibco-BRL, Life Technologies) containing 10 % fetal bovine serum (Invitrogen, Life Technologies), glutamine (2 millimol l^{-1}), and Gibco Antibiotic–Antimycotic solution (Gibco-BRL) and incubated at 37 °C in an atmosphere of 5 % CO_2. After isolation, partial trypsinizations have been carried out in order to separate primary PTC cells from all other contaminating cells, according to previously published protocols [19, 20]. In addition, primary tumor cells were negatively selected using magnetic anti-fibroblast beads (Miltenyi Biotec GmbH, Germany) after the first passage, according to manufacturer's instructions. The isolated primary cultures have been maintained from 1 week to 4 weeks prior to switch them to the CSC medium.

To obtain thyrospheres, primary cell lines were seeded at a density of 3×10^6 cells into low adhesion flasks (25 cm^2) (Corning, NY, USA) containing CSC medium [DMEM/F12, glutamine (2 millimol l^{-1})], Gibco Antibiotic–Antimycotic solution, and a mixture of hormones [21, 22]. The medium was supplemented with epidermal growth factor (EGF) (20 ng/ml) and basic fibroblast growth factor (bFGF) (20 ng/ml), both obtained from Sigma-Aldrich Chemicals. Before experiments, the absence of mycoplasma in each cell line was verified with the EZ-PCR Mycoplasma Test Kit (Biological Industries, Israel Beit-Haemek LTD, Israel).

Self-renewal capability for three lines was determined using extreme limiting dilution analysis (ELDA, an online tool for limiting dilution analysis; http://bioinf.wehi.edu.au/software/elda/) (data not shown).

ALDEFLUOR assay and flow cytometry

Aldehyde dehydrogenase (ALDH) activity was assessed in samples ($2x10^4$ cells) of four cell lines using the ALDEFLUOR kit (StemCell Technologies, Vancouver, Canada). Intracellular fluorescence was measured by flow cytometry

(FACS Canto and FACSAria, Becton–Dickinson, San Jose, CA, for analysis and sorting, respectively). Sorting gates were established based on the results of negative controls consisting of cells pretreated with the specific ALDH inhibitor diethylaminobenzaldehyde (DEAB).

Total protein extraction for assessment of pluripotency biomarker expression and RTK phosphorylation

Thyrospheres and primary cell culture pellets were lysed in 40 µl of lysis buffer containing TrisHCl (pH 7.4, 50 millimol l^{-1}), NaCl (150 millimol l^{-1}), Triton (1 % v/v), ethylenediaminetetraacetic acid (EDTA, 20 millimol l^{-1}), phenylmethylsulfonyl fluoride (PMSF, 2 millimol l^{-1}), protease and phosphatase inhibitors (2X), leupeptin (2 µg/ml), glycerol (10 % v/v), and water. Total protein was extracted on ice and quantified with the BCA Protein Assay (Pierce, Rockford, IL, USA). Results were read in a Nanodrop2000 spectrophotometer (Thermo Scientific).

The lysate was then assayed with the Human Pluripotent Stem Cell Array and Human Phospho-RTK array kits (both from R&D Systems, Minneapolis, MN). Stem cell markers (i.e., Oct3/4; Nanog; SOX2; E-chaderin; Gata-4; FoxA2; IPF1; SOX17; Otx2; TP63; Goosecoid; Snail1; VEGFR2; HCG; AFP) and phosphorylated RTKs were detected using chemiluminescence western blotting with Clarity Western ECL substrate (BIO-RAD) and a charge-coupled device camera (Chemidoc, BIO-RAD, Hercules, CA, USA).

RNA extraction, RT-PCR, and screening with the TaqMan Low Density Array (TLDA)

RNA was extracted from primary cell cultures and thyrospheres with the RNeasy Mini Kit (Qiagen, Venlo, Netherlands). Its concentration and purity were assessed by measuring the optical density (OD) at 260 and 280 nm with a Nanodrop 2000 spectrophotometer.

Total RNA was reverse transcribed using the High Capacity cDNA Reverse Transcription kit (Life Technologies). One hundred nanograms of each cDNA were used as a template for analysis with the real-time PCR-based custom TaqMan Low Density Array (TLDA, Life Technologies), which contains specific predesigned assays for expression levels of 48 genes (TaqMan Gene Expression Assays, Life Technologies), including thyroid-specific differentiation markers and key genes involved in the EMT. Four housekeeping genes (*ACTB*, *B2 M*, *GAPDH*, and *HRPT1*) were included in each array to normalize raw data. The reaction set-up and amplification in the ABI PRISM 7900HT Sequence Detection System (Life Technologies) have been described elsewhere [23].

Cell proliferation and RTK phosphorylation after exposure to crizotinib

For proliferation assays, cells were seeded into 96-well plates in quadruplicate and treated for 48 h with crizotinib (PF-2341066 purchased from Selleck, Houston, TX) at concentrations of 1 and 10 micromol l^{-1} (in DMSO) or with DMSO alone, as described in Zhou et al. [24]. Proliferation was evaluated with the alamarBlue® (AB) assay (Life Technologies). Samples of the primary cultures and their CSC subsets were seeded into 96-well plates (5×10^3 and 10×10^3 cells/well, respectively), and AB was added directly to the culture medium (final concentration: 10 % v/v). After 24, 48, and 72 h of incubation, the OD of the plate was measured at 550 and 620 nm with a standard spectrophotometer. As a negative control, AB was added to the medium without cells. The half maximal inhibitory

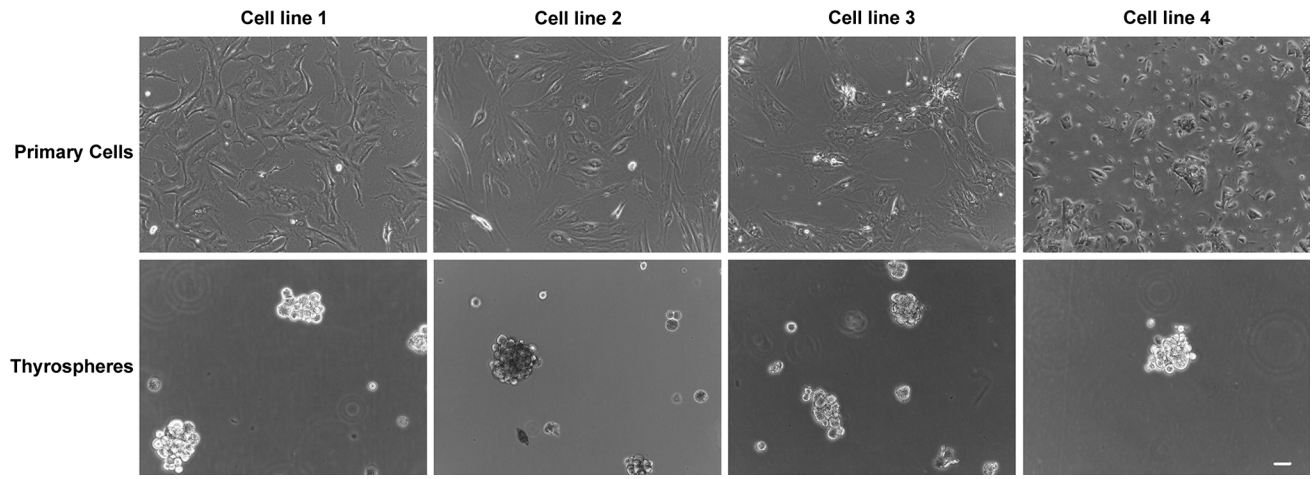

Fig. 1 Phase-contrast images of primary thyroid cancer *cell lines 1–4* and the thyrospheres derived from each cell line. Primary cell lines were established from 4 aggressive thyroid cancers. The thyrospheres were derived from primary cultures after 1 week of growth in stem cell medium supplemented with EGF and bFGF. *Scale bar* 200 µM

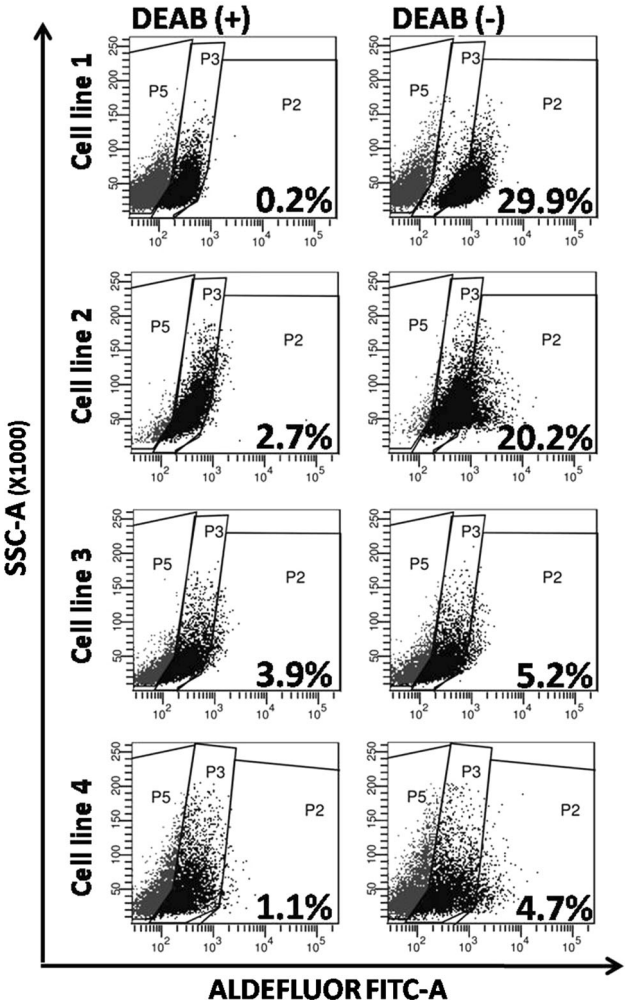

Fig. 2 Aldehyde dehydrogenase activity in primary *cell lines 1–4*. ALDH activity was measured with the Aldefluor assay. *Left-hand panels* The ALDH inhibitor DEAB was added to each sample before staining, as a control for background fluorescence. Results were used to confirm the gating area. *Right-hand panels* Samples assayed without DEAB pretreatment. P2, P3, and P5: Cell populations with high, intermediate, and low ALDH activity, respectively. The percentage of P2 ($ALDH^{high}$) is reported in the lower right corner of each graph. *x*-axis: intensity of emitted fluorescence expressed on a logarithmic scale; *y*-axis: cell size (side scatter or SSC)

concentration (IC_{50}) values were evaluated by nonlinear regression analysis with Prism 5.04 (GraphPad Software, La Jolla, CA). The number of viable cells correlates with the magnitude of dye reduction. Results were expressed as percentage of AB reduction [25] after correction for background values observed in negative controls.

For Human Phospho-RTK array analysis, cells were seeded into 6-well plates and treated for 48 h with crizotinib at concentrations of 0.05 micromol l^{-1} (primary line 1), 0.2 micromol l^{-1} (primary line 2), 1 micromol l^{-1} (primary line 4), and 1.5 micromol l^{-1} (CSC lines 1, 2, and 4).

Data analysis

Human Pluripotent Stem Cell Array results were analyzed with MyImage Analysis software (Thermo Scientific Inc, Rockford, IL USA). Human Phospho-RTK array results were analyzed using ImageLab software (Chemidoc BIO-RAD). In both cases, the signal of each spot was normalized to the mean signal of the negative controls (background) present on the membrane.

Expression Suite software (Life Technologies) was used for gene expression analysis with the comparative Ct ($\Delta\Delta$Ct) method and for assessing the expression of the target genes normalized to a calibrator (primary cancer cells). The *ACTB* gene was used to normalize data because of its low variation among the samples. The detection threshold was set at 35. Data are expressed as means (SD). Statistical significance was assessed with the Student's *t* test, and results were considered significant when *P* values were <0.05.

Results

Thyrosphere formation

Primary cell lines were established from three poorly differentiated thyroid cancers (primary tumor—line 4; locally recurrent lesion—line 2; lymph node metastasis—line 1) and one follicular-variant papillary thyroid cancer (lymph node metastasis—line 3). The clinical, pathological, and genetic characteristics of each case are reported in Supplementary Table 1 and Supplemental Fig. 1. After three passages, 3×10^6 cells of each line were cultured under stem-like conditions to allow selective proliferation of immature tumor cells. Within 24 h, thyrosphere formation was observed as the organization of small aggregates of cells floating in suspension (Fig. 1). The thyrospheres were maintained for at least 1 month. When plated under the same conditions, cells dissociated from the spheres generated secondary thyrospheres (data not shown), thus demonstrating their capacity for self-renewal.

Assessment of stem cell-like properties

ALDH activity

Because enhanced ALDH activity appears to be a hallmark of CSCs [26–28], the four primary thyroid cancer cell lines were subjected to ALDEFLUOR assay by FACS analysis (Fig. 2). The percentage of $ALDH^{high}$ cells varied widely (4.7–29.9 %), with higher figures recorded in cell lines 1 and 2 than in those derived from cell line 3 or cell line 4.

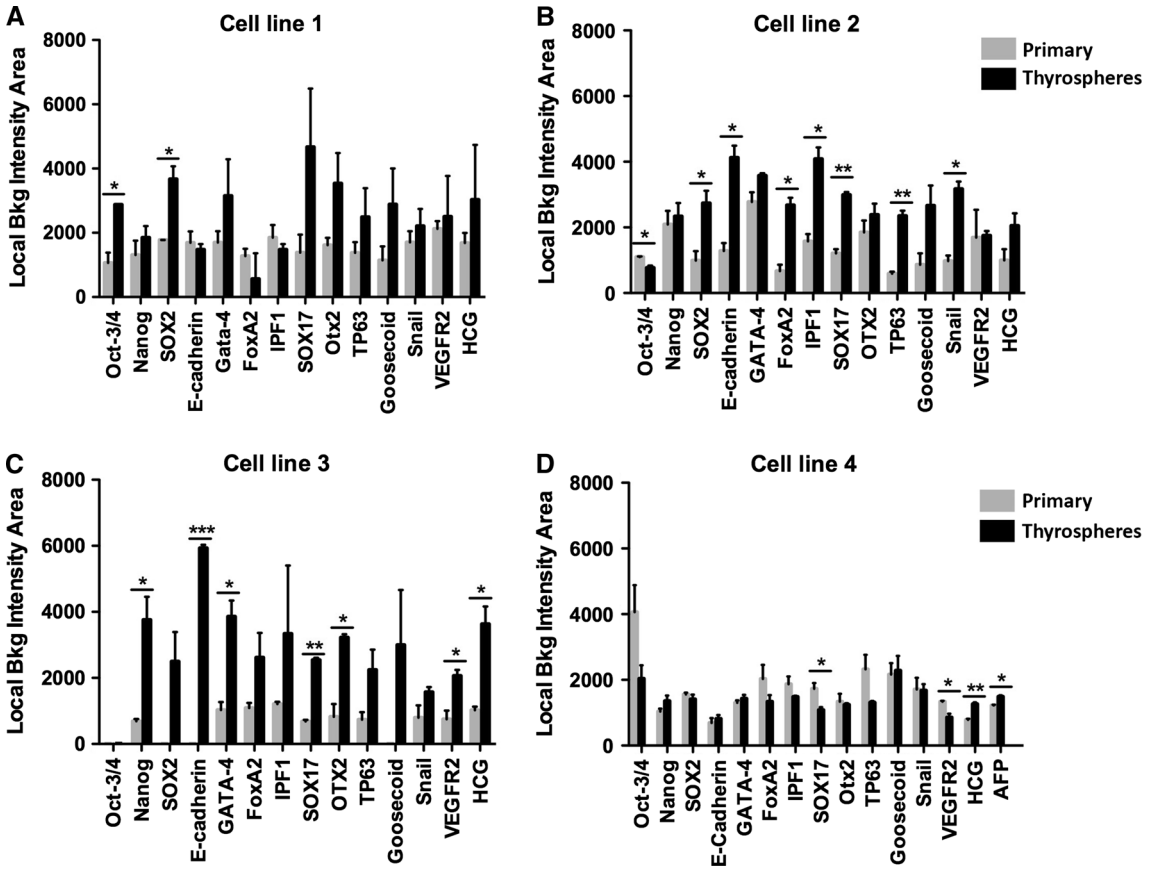

Fig. 3 Expression of pluripotency-related proteins by thyrosphere cells. Expression levels of pluripotency markers were measured in total cell extracts with the Proteome Profiler Human Pluripotent Stem Cell Array kit. Thyrosphere cells were tested after 1 week's growth under stem cell conditions and results compared with those obtained in primary cell cultures from the same tumor. Differences were assessed with the Student's *t* test (*$p < 0.05$; **$p < 0.01$; ***$p < 0.001$). Data are expressed as background- and area-normalized pixel intensity. *Error bars* represent standard deviation

These data suggest that ALDH activity is restricted to a subpopulation of cells of the thyroid tumors characterized by substantial individual variability.

Expression of stem cell markers

We decided to further analyze the expression of several stem cell markers in the unsorted thyrosphere cell populations. Total protein extracts from primary cultures and from thyrosphere cells grown for 1 week under stem cell-like conditions were thus assayed for the expression of 15 established markers of pluripotency with the Human Pluripotent Stem Cell Array Kit.

The expression level of each marker varied substantially from one cell line to another. Thyrospheres from cell line 1 displayed significant overexpression of markers Oct3/4 and SOX2 relative to the primary cell line derived from the same tumor (Fig. 3a). Significant differential expression in thyrosphere cells was more common in cell line 2, involving seven markers with upregulated expression (SOX2, E-cadherin, FoxA2, IPF1, SOX17, TP63, and Snail), and 1 (Oct3/4) that was downregulated relative to primary cultures (Fig. 3b). In cell line 3, three stem cell markers were expressed exclusively in the thyrosphere cells (SOX2, GOOSECOID, and E-CADHERIN), and six others (Nanog, GATA-4, SOX17, OTX2, VEGFR2, and HCG) were significantly overexpressed in these cells, as compared with primary tumor cells (Fig. 3c). As for cell line 4, significant differences between thyrosphere and primary cells were found for only two of the 15 markers (HCG and AFP), both of which were overexpressed in thyrospheres (Fig. 3d).

These data are fully consistent with the inter-tumor variability of thyrosphere populations highlighted by the ALDEFLUOR assay data. The significant increase in the expression of pluripotency markers, and in particular of SOX2, under stem cell culture conditions supports the identification of thyrosphere cells of all four cell lines as CSCs.

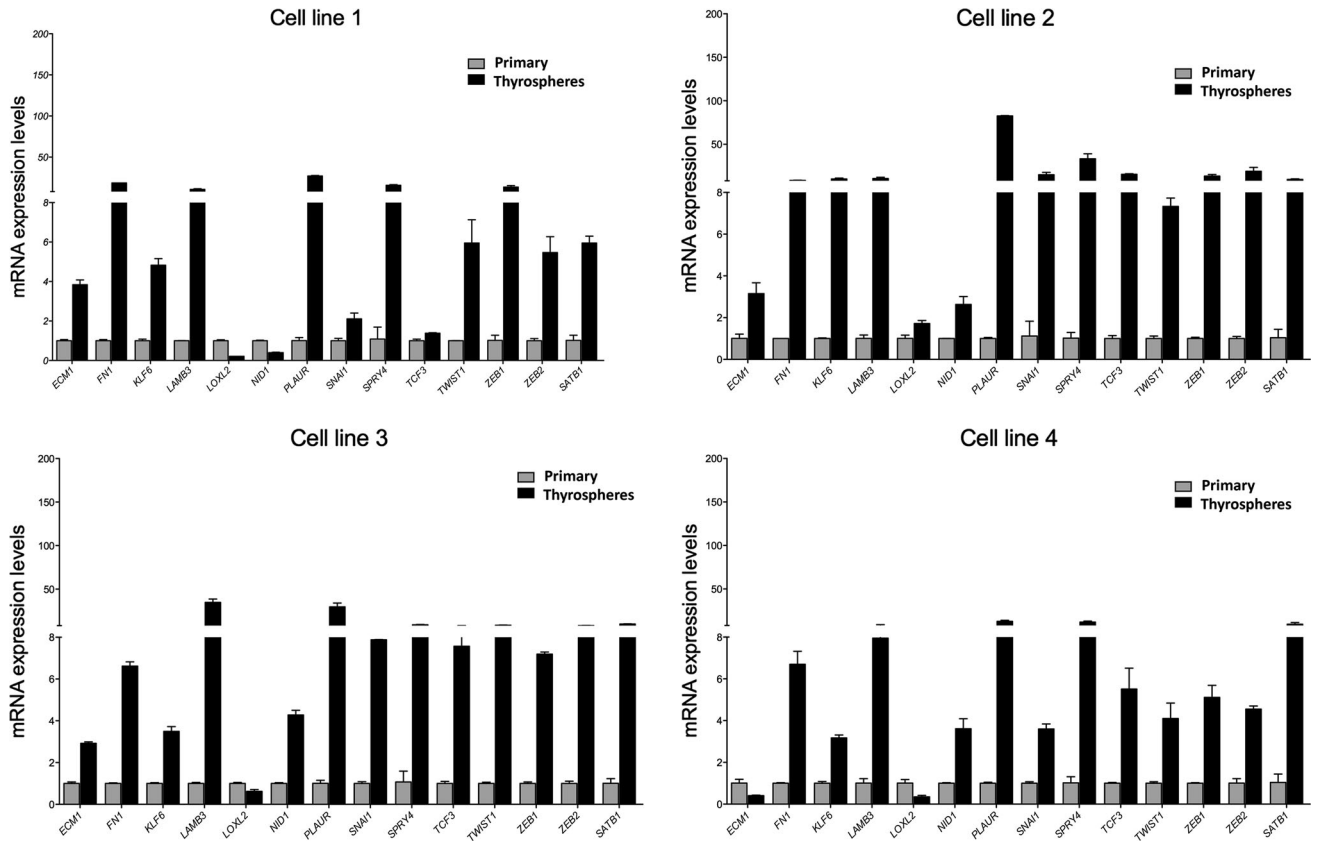

Fig. 4 EMT-related genes exhibiting significant differential expression in thyrospheres and primary cell populations from all 4 tumors. Columns (*error bars*) represent means (±SD) of two samples tested with TLDA. Differences between thyrosphere expression levels and those of corresponding primary cells (calibrator) were assessed with the Student *t* test ($p < 0.05$ in all cases)

Differential expression of EMT-related genes in thyrospheres

The TaqMan Low Density Array (Life Technologies) was used to comparatively analyze the expression of genes involved in thyroid differentiation and those considered markers of the EMT in thyrospheres and primary cell cultures from each of the four cancers. As expected, given the poorly differentiated status of the tissues, all of the cells analyzed (primary cultures and thyrospheres) were characterized by undetectable levels of *NIS*, *TSHR,* and *TPO* transcript and very low levels of *TG*, *TTF1*, and *PAX8* mRNA (Supplemental Fig. 3). Comparative analysis (thyrospheres *vs* primary tumor cells) revealed sometimes higher expression of the last three genes. This behavior could be not surprising considering their early expression also in embryogenesis [29]. The EMT-related gene expression profiles of the four cell lines are reported in full in both Supplemental Table 2 and Supplemental Fig. 2. Fourteen genes displayed significant differential expression (upregulation, in most cases) in all four CSC populations (vs. the primary cell cultures) of all four lines (Fig. 4).

RTK phosphorylation patterns in primary and thyrosphere populations

Next, to identify potential therapeutic targets, we assessed phosphorylation levels of six RTKs known to be EMT-related [30–33] in thyrosphere and primary tumor cell populations. This analysis was restricted to cell lines 1, 2, and 4; cell line 3 was excluded from this and subsequent analyses because the thyrosphere population had been exhausted in the previous experiments.

Figure 5 shows the RTKs found to be activated in the primary and thyrosphere populations of each cell line. The results varied widely from one cell line to another. In line 1, ALK and EGFR showed high phosphorylation levels in both thyrospheres and primary cultures (Fig. 5a). In line 2, five of the six RTKs assessed were highly phosphorylated in primary culture cells and less phosphorylated in the thyrosphere populations (Fig. 5b). In line 4, all RTKs assessed were substantially phosphorylated in the primary cultures and thyrosphere populations, an increase in the phosphorylation levels of DTK were however noted in thyrosphere line 4 (Fig. 5c). These data indicate the

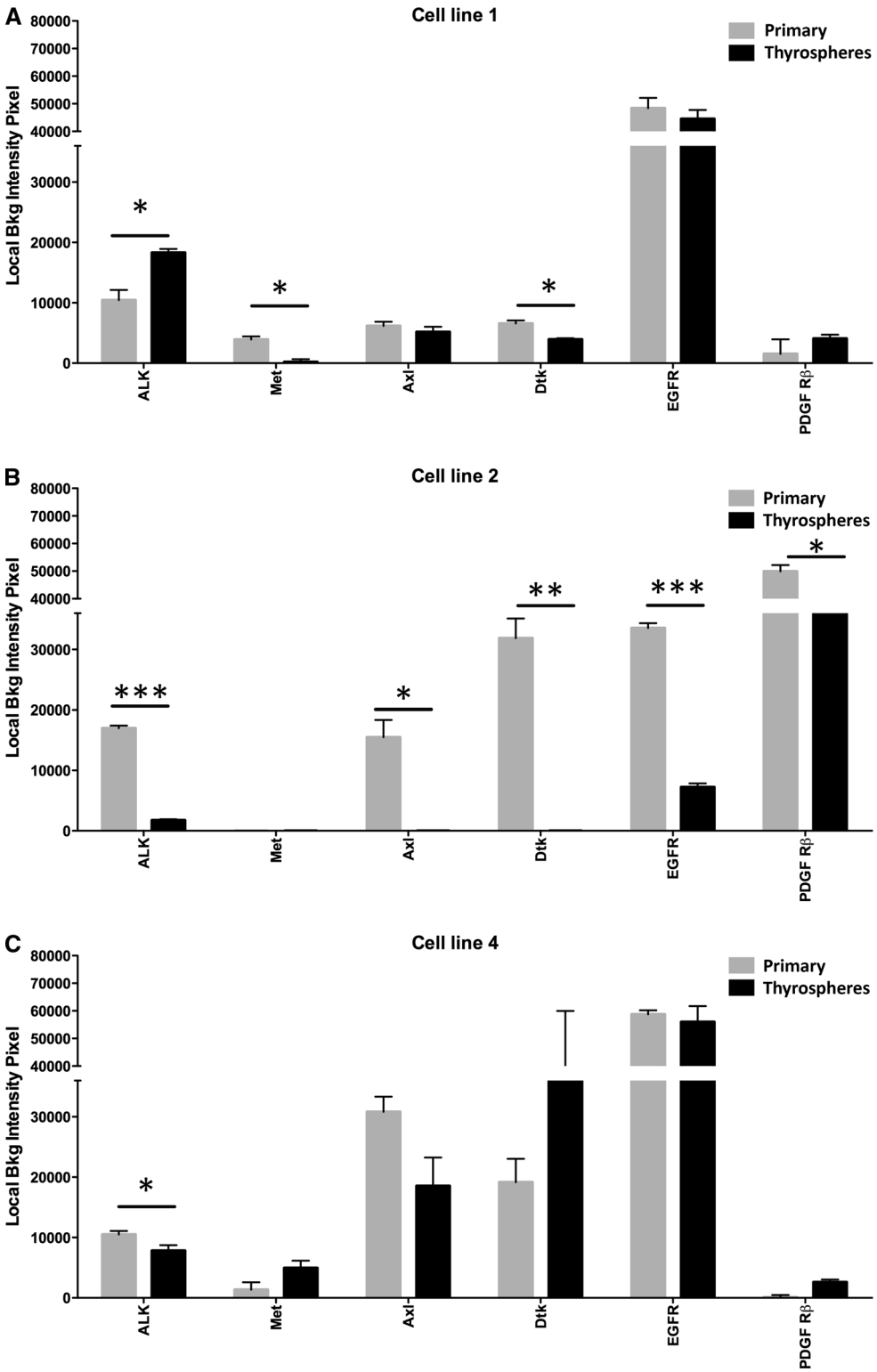

Fig. 5 Receptor tyrosine kinase (RTK) phosphorylation levels in thyrosphere populations. RTK phosphorylation levels were measured in total protein extracts with the Human Phospho-RTK Array. Results are shown for primary and CSC lines representing tumors 1, 2, and 4. RTKs represented are those known to be involved in the EMT process. Data are expressed as background-normalized pixel intensity. *Error bars* represent standard deviation. Statistical significance was assessed with the Student's *t* test (*$p < 0.05$; **$p < 0.01$; ***$p < 0.001$)

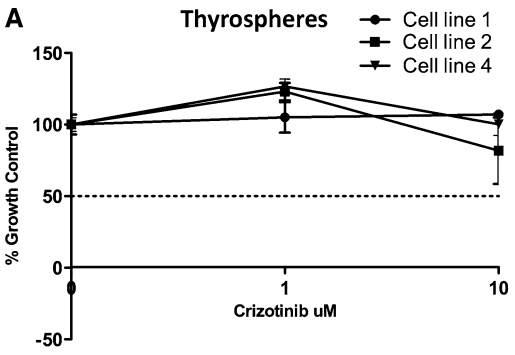

Cell Lines	Drug	$IC_{50}\mu M$
Thyrospheres 1	Crizotinib	resistant
Thyrospheres 2	Crizotinib	resistant
Thyrospheres 4	Crizotinib	resistant

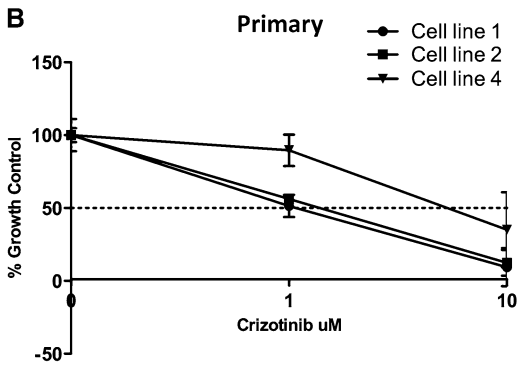

Cell Lines	Drug	$IC_{50}\mu M$
Primary 1	Crizotinib	0.009-0.4
Primary 2	Crizotinib	0.55-1
Primary 4	Crizotinib	1.5-10

Fig. 6 Effect of crizotinib exposure on proliferation of primary *cell lines 1*, *2*, and *4* and their corresponding thyrosphere cells. Percentage of growth inhibition observed in thyrosphere lines (**a**) and primary cell lines (**b**) after 48 h exposure to crizotinib at concentrations of 1 micromol l^{-1} and 10 micromol l^{-1}. *Curves* correspond to a representative results of experiments performed in triplicate. The table below each graph summarizes the IC_{50} of crizotinib calculated on the basis of three independent experiments

activation of specific RTK in each cell line; moreover, in primary and thyrosphere subsets from all three lines, at least one EMT-related RTK was highly activated.

Effect of crizotinib on the proliferation of primary culture cells and thyrospheres

Given the dysregulation of EMT-related genes and the RTK phosphorylation levels observed in the three thyroid cancer cell lines, we decided to evaluate the responses of these cells to the multiple tyrosine kinase inhibitor crizotinib [34, 35].

Thyrosphere viability in lines 1, 2, and 4 was investigated after 48 h of exposure to crizotinib concentrations ranging from 1 to 10 micromol l^{-1} (as previously described in [24]) and the half maximal inhibitory concentration (IC_{50}) calculated for each line. As shown in Fig. 6, proliferation of CSCs from lines 1, 2 and 4 was not significantly inhibited, even by the maximal dose tested (Fig. 6a). In contrast, cells from the primary cultures of lines 1, 2, and 4 (Fig. 6b) were all sensitive to treatment with crizotinib with IC_{50} ranging from 9 to 10 micromol l^{-1}.

The responses observed in these experiments might be attributed to the different RTK activation patterns observed in the three cell lines. To explore this possibility, we analyzed the inhibitory activity of crizotinib on the phosphorylation of nine RTKs that were EMT-related and/or known crizotinib targets in cell lines 1, 2, and 4 (primary cultures and thyrospheres). The crizotinib concentrations used in these experiments were approximately one-fourth the IC_{50} values shown in Fig. 6. As in previous experiments, the responses of the three cell lines were appreciably different (Fig. 7). In cells from all three primary cultures, crizotinib decreased the phosphorylation of ALK, a known target of the drug (Fig. 7a–c). As for the thyrosphere, line 1 responded to crizotinib treatment with upregulated phosphorylation of RTKs known to be direct targets of the drug (i.e., TRKA, TRKB, and AXL) (Fig. 7d); thyrosphere line 2 displayed an increase of phosphorylation levels of all the targets of crizotinib assessed, a downregulated phosphorylation of PDGFRB (which is not a direct target of the drug), as well as a huge increase of EGFR phosphorylation (Fig. 7e). As for the thyrosphere, line 4 displayed significant post-treatment downregulation of PDGFRB phosphorylation, together with a very substantial decrease in DTK phosphorylation (Fig. 7f).

Discussion

Treatment of radiorefractory thyroid cancer is still an unresolved issue and elucidation of the cellular pathways involved in the tumorigenic process may help to choose a more appropriate targeted treatment [36].

In the present study, we established primary cell cultures from four aggressive, ^{131}I-refractory thyroid cancers and obtained cells with stem cell properties to analyze functional features of this cell subset. The thyrospheres varied widely in terms of their stem cell marker profiles. All,

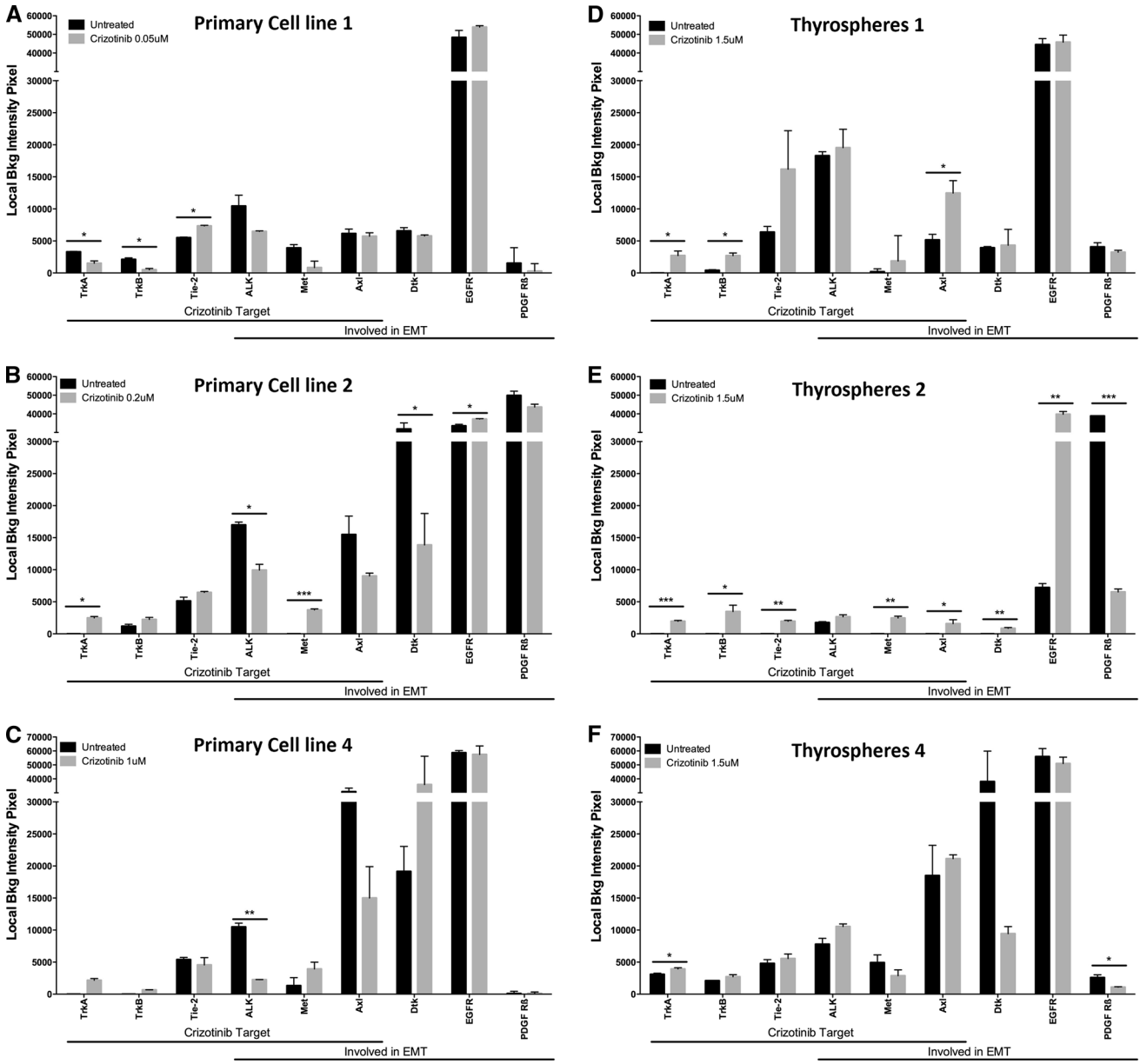

Fig. 7 Effect of crizotinib exposure on RTK phosphorylation in primary *cell lines 1*, *2*, and *4* and their corresponding thyrosphere cells. RTK phosphorylation levels were measured after 48 h exposure to crizotinib in primary cell cultures (concentrations: 0.05 micromol l^{-1} in line 1, 0.2 micromol l^{-1} in line 2, and 1 micromol l^{-1} in line 4) (**a–c**) and thyrosphere cells (**d–f**) at a concentration of 1.5 micromol l^{-1}. Data are expressed as background-normalized pixel intensity. *Error bars* represent standard deviation. Statistical significance was assessed with the Student's *t* test ($*p < 0.05$; $**p < 0.01$; $***p < 0.001$)

however, were characterized by upregulated expression of several EMT-related genes with respect to that observed in the primary cells from the same tumors. As for EMT-related RTKs (PDGFRB, ALK, MET, AXL, DTK, EGFR), at least one was activated in the three thyrosphere line tested, although on the whole they displayed less activated RTKs than primary cells. This behavior could be probably addressed to a quiescent or slow-cycling state of thyrosphere cells as compared to primary tumor cells. The molecular profiles of the CSC-enriched population also varied widely from one tumor subtype to another, and differences were even observed between tumors of the same subtype. Although the number of tumors analyzed in our study was admittedly limited, our data suggest that the factors sustaining the pluripotency of thyrospheres differ with the tumor histotype. In fact, the expression of SOX2 and SOX17 was significantly upregulated in thyrospheres 1, 2, and 3 (relative to primary cells). However, no significant difference was observed between SOX2 expression levels in primary and CSC lines from tumor 4, and SOX17

expression was actually downregulated in the thyrospheres subset. SOX2 upregulation has been reported in several types of adult stem/progenitor cells and a variety of malignant tumors, where it can promote tumor growth even in the absence of Oct4 [37–40]. In a more recent study [41], downregulation of SOX2 in a human undifferentiated thyroid cancer cell line rendered the cells sensitive to cisplatin and doxorubicin treatment. As for SOX17, it seems to be involved in a switch that converts the Oct4 complex from a pluripotency regulator to an endodermal gene activator [42, 43].

Although TLDA analysis revealed marked variability between the thyrospheres in terms of gene expression profiles, all four were characterized by overexpression of many important EMT-related genes relative to the primary cell lines, which supports the view that the stem cell properties of thyrospheres are closely related to the EMT.

One of the cardinal features of the EMT is the loss of expression of adhesion molecules, which allows tumor cells to detach from and migrate away from the primary tumor site [8]. In two of the four thyrosphere lines we tested (lines 2 and 3), however, expression of the adhesion molecule E-cadherin was significantly upregulated rather than downregulated relative to the corresponding primary tumor cell lines. Chao et al. have noted that E-cadherin expression is largely restored in cells that have already metastasized. In this context, it is thus interesting to note that lines 2 and 3 were both derived from secondary lesions (see Supplementary Table 1) [44, 45].

CSC lines 1, 2, and 4 were characterized by the activation of several EMT-related RTKs that are known to be direct targets of crizotinib. Although our CSC line cell viability was not significantly inhibited after exposure to the drug, proliferation of all the primary cell cultures was reduced by nanomolar to micromolar concentrations of crizotinib. The discrepancy between crizotinib's effects in our primary thyroid cancer cell lines and the CSC sub-populations of these lines is suggestive of a phenomenon of resistance to the drug in a subpopulation of each tumor. Although the majority of the cells in the tumor mass are inhibited by the drug, the thyrospheres remain unresponsive likely thanks to their distinctive RTK activation profiles. Subsequent selection of these cells may lead to disease recurrence and/or progression. "Switching off" a few of the kinases activated in these cells (possibly even one) may be sufficient to counteract this resistance, as previously demonstrated in other cancers [46–48]. Accordingly, the concept of "combination therapy" is increasingly relevant in treatment of aggressive thyroid carcinoma [49].

In conclusion, our findings highlight the variability of CSC populations from different tumors. They also support the role played by the EMT process in thyrospheres and the hypothesis that thyrospheres are involved in thyroid cancer progression and their resistance to treatment. In our study, the lack of other experimental models as well as the reduced number of samples analyzed constituted a limitation in identifying some more complicated molecular mechanisms of drug resistance.

Tailored approaches are needed for the management of poorly differentiated/metastatic thyroid cancers that are refractory to conventional therapies. Ongoing attempts to characterize the molecular profiles of CSCs from individual thyroid cancers will provide insight into the process of thyroid carcinogenesis and potentially useful information for developing individualized targeted therapies for these tumors.

Acknowledgments This study was funded by grants from the Italian Ministry of Universities and Research (FIRB 2008—number RBFR082XL7_003 to C.D., MIUR/Cofin 2010-2011 to D.R.) and from the Fondazione Umberto Di Mario ONLUS. The manuscript was edited by Marian Everett Kent, BSN.

Compliance with ethical standards

Conflict of interest The authors declare that there is no conflict of interest that could be perceived as prejudicing the impartiality of the research reported.

References

1. C. Durante, N. Haddy, E. Baudin, S. Leboulleux, D. Hartl, J.P. Travagli, B. Caillou, M. Ricard, J.D. Lumbroso, F. De Vathaire et al., Long-term outcome of 444 patients with distant metastases from papillary and follicular thyroid carcinoma: benefits and limits of radioiodine therapy. J. Clin. Endocrinol. Metab. **91**, 2892–2899 (2006)
2. M. Schlumberger, L. Lacroix, D. Russo, S. Filetti, J.M. Bidart, Defects in iodide metabolism in thyroid cancer and implications for the follow-up and treatment of patients. Nat. Clin. Pract. Endocrinol. Metab. **3**, 260–269 (2007)
3. F. Arturi, D. Russo, D. Giuffrida, M. Schlumberger, S. Filetti, Sodium–iodide symporter (NIS) gene expression in lymph-node metastases of papillary thyroid carcinomas. Eur. J. Endocrinol. **143**, 623–627 (2000)
4. F. Arturi, D. Russo, J.M. Bidart, D. Scarpelli, M. Schlumberger, S. Filetti, Expression pattern of the pendrin and sodium/iodide symporter (NIS) gene in human thyroid carcinoma cell lines and human thyroid tumors. Eur. J. Endocrinol. **145**, 129–135 (2001)
5. T. Kogai, G.A. Brent, The sodium iodide symporter (NIS): regulation and approaches to targeting for cancer therapeutics. Pharmacol. Ther. **135**, 355–370 (2013)
6. D. Russo, G. Damante, E. Puxeddu, C. Durante, S. Filetti, Epigenetics of thyroid cancer and novel therapeutic targets. J. Mol. Endocrinol. **46**, R73–R81 (2011)
7. M. Xing, Molecular pathogenesis and mechanisms of thyroid cancer. Nat. Rev. Cancer **13**, 184–199 (2013)
8. J.P. Thiery, Epithelial-mesenchymal transitions in tumour progression. Nat. Rev. Cancer **2**, 442–454 (2002)
9. T. Reya, S.J. Morrison, M.F. Clarke, I.L. Weissman, Stem cells, cancer, and cancer stem cells. Nature **414**, 105–111 (2001)
10. T. Brabletz, A. Jung, S. Spaderna, F. Hlubek, T. Kirchner, Migrating cancer stem cells—an integrated concept of malignant tumour progression. Nat. Rev. Cancer **5**, 744–749 (2005)

11. Z. Guo, H. Hardin, R.V. Lloyd, Cancer stem-like cells and thyroid cancer. Endocr. Relat. Cancer **21**, T285–T300 (2014)
12. H. Hardin, C. Montemayor-Garcia, R.V. Lloyd, Thyroid cancer stem-like cells and epithelial-mesenchymal transition in thyroid cancers. Hum. Pathol. **44**, 1707–1713 (2013)
13. M. Todaro, F. Iovino, V. Eterno, P. Cammareri, G. Gambara, V. Espina, G. Gulotta, F. Dieli, S. Giordano, R. De Maria, G. Stassi, Tumorigenic and metastatic activity of human thyroid cancer stem cells. Cancer Res. **70**, 8874–8885 (2010)
14. Y. Qin, C. Capaldo, B.M. Gumbiner, I.G. Macara, The mammalian Scribble polarity protein regulates epithelial cell adhesion and migration through E-cadherin. J. Cell Biol. **171**, 1061–1071 (2005)
15. S.A. Mani, W. Guo, M. Liao, E.N. Eaton, A.Y. Zhou, M. Brooks, F. Reinhard, C.C. Zhang, L.L. Campbell, K. Polyak, C. Brisken, J. Yang, R.A. Weinberg, The epithelial-mesenchymal transition generates cells with properties of stem cells. Cell **133**, 704–715 (2008)
16. Thyroid American Joint Committee on Cancer 2002: AJCC Cancer Staging Man. pp. 77–87 (2010)
17. M.D. Castellone, A. Verrienti, D. Magendra Rao, M. Sponziello, D. Fabbro, M. Muthu, C. Durante, M. Maranghi, G. Damante, S. Pizzolitto, G. Costante, D. Russo, M. Santoro, S. Filetti, A novel de novo germ-line V292M mutation in the extracellular region of RET in a patient with phaeochromocytoma and medullary thyroid carcinoma: functional characterization. Clin. Endocrinol. **73**, 529–534 (2010)
18. F. Rosignolo, V. Maggisano, M. Sponziello, M. Celano, C.R. Di Gioia, M. D'Agostino, L. Giacomelli, A. Verrienti, M. Dima, V. Pecce, C. Durante, Reduced expression of THRβ in papillary thyroid carcinomas: relationship with BRAF mutation, aggressiveness and miR expression. J. Endocrinol. Invest. (2015). doi:10.1007/s40618-015-0309-4
19. L. Khandrika, F.J. Kim, A. Campagna, S. Koul, R.B. Meacham, H.K. Koul, Primary culture and characterization of human renal inner medullary collecting duct epithelial cells. J. Urol. **179**, 2057–2063 (2008)
20. A. Hague, C. Paraskeva, The intestinal epithelial cell, in *Epithelial Cell Culture*, ed. by A. Harris (Cambridge University Press, New York, 1996), pp. 25–41
21. L. Ricci-Vitiani, D.G. Lombardi, E. Pilozzi, M. Biffoni, M. Todaro, C. Peschle, R. De Maria, Identification and expansion of human colon-cancer-initiating cells. Nature **445**, 111–115 (2007)
22. M. Todaro, M.P. Alea, A.B. Di Stefano, P. Cammareri, L. Vermeulen, F. Iovino, C. Tripodo, A. Russo, G. Gulotta, J.P. Medema, G. Stassi, Colon cancer stem cells dictate tumor growth and resist cell death by production of interleukin-4. Cell Stem Cell **1**, 389–402 (2007)
23. M. Sponziello, E. Lavarone, E. Pegolo, C. Di Loreto, C. Puppin, M. Russo, R. Bruno, S. Filetti, C. Durante, D. Russo, A. Di Cristofano, G. Damante, Molecular differences between human thyroid follicular adenoma and carcinoma revealed by analysis of a murine model of thyroid cancer. Endocrinology. **154**, 3043–3053 (2013)
24. Y. Zhou, C. Zhao, S. Gery, G.D. Braunstein, R. Okamoto, R. Alvarez, S.A. Miles, N.B. Doan, J.W. Said, J. Gu, H. Phillip Koeffler, Off-target effects of c-MET inhibitors on thyroid cancer cells. Mol. Cancer Ther. **13**, 134–143 (2014)
25. M.M. Nociari, A. Shalev, P. Benias, C. Russo, A novel one-step, highly sensitive fluorometric assay to evaluate cell-mediated cytotoxicity. J. Immunol. Methods **213**, 157–167 (1998)
26. E.H. Huang, M.J. Hynes, T. Zhang, C. Ginestier, G. Dontu, H. Appelman, J.Z. Fields, M.S. Wicha, B.M. Boman, Aldehyde dehydrogenase 1 is a marker for normal and malignant human colonic stem cells (SC) and tracks SC overpopulation during colon tumorigenesis. Cancer Res. **69**, 3382–3389 (2009)
27. J.L. Dembinski, S. Krauss, Characterization and functional analysis of a slow cycling stem cell-like subpopulation in pancreas adenocarcinoma. Clin. Exp. Metastasis **26**, 611–623 (2009)
28. C. van den Hoogen, G. van der Horst, H. Cheung, J.T. Buijs, J.M. Lippitt, N. Guzmán-Ramírez, F.C. Hamdy, C.L. Eaton, G.N. Thalmann, M.G. Cecchini, R.C.M. Pelger, G. van der Pluijm, High aldehyde dehydrogenase activity identifies tumor-initiating and metastasis-initiating cells in human prostate cancer. Cancer Res. **70**, 5163–5173 (2010)
29. L.P. Fernández, A. López-Márquez, P. Santisteban, Thyroid transcription factors in development, differentiation and disease. Nat. Rev. Endocrinol. **11**, 29–42 (2015)
30. H.R. Kim, W.S. Kim, Y.J. Choi, C.M. Choi, J.K. Rho, J.C. Lee, Epithelial-mesenchymal transition leads to crizotinib resistance in H2228 lung cancer cells with EML4-ALK translocation. Mol. Oncol. **7**, 1093–1102 (2013)
31. S. Thomson, F. Petti, I. Sujka-Kwok, P. Mercado, J. Bean, M. Monaghan, S.L. Seymour, G.M. Argast, D.M. Epstein, J.D. Haley, A systems view of epithelial–mesenchymal transition signaling states. Clin. Exp. Metastasis **28**, 137–155 (2010)
32. C. Holz, F. Niehr, M. Boyko, T. Hristozova, L. Distel, V. Budach, I. Tinhofer, Epithelial-mesenchymal-transition induced by EGFR activation interferes with cell migration and response to irradiation and cetuximab in head and neck cancer cells. Radiother. Oncol. **101**, 158–164 (2011)
33. I. Cañadas, F. Rojo, Á. Taus, O. Arpí, M. Arumí-Uría, L. Pijuan, S. Menéndez, S. Zazo, M. Dómine, M. Salido, S. Mojal, A. García de Herreros, A. Rovira, J. Albanell, E. Arriola, Targeting epithelial-to-mesenchymal transition with Met inhibitors reverts chemoresistance in small cell lung cancer. Clin. Cancer Res. **20**, 938–950 (2014)
34. H.Y. Zou, Q. Li, J.H. Lee, M.E. Arango, S.R. McDonnell, S. Yamazaki, T.B. Koudriakova, G. Alton, J.J. Cui, P.P. Kung, M.D. Nambu, G. Los, S.L. Bender, B. Mroczkowski, J.G. Christensen, An orally available small-molecule inhibitor of c-Met, PF-2341066, exhibits cytoreductive antitumor efficacy through antiproliferative and antiangiogenic mechanisms. Cancer Res. **67**, 4408–4417 (2007)
35. Drug Evaluation: Center for Drug Evaluation and Pharmacology Review (S). http://www.accessdata.fda.gov/drugsatfda_docs/nda/2011/202570Orig1s000PharmR.pdf (2011)
36. U. Hinterseher, A. Wunderlich, S. Roth, A. Ramaswamy, D.K. Bartsch, S. Hauptmann, B.H. Greene, V. Fendrich, S. Hoffmann, Expression of hedgehog signalling pathway in anaplastic thyroid cancer. Endocrine **45**, 439–447 (2014)
37. S.M. Rodriguez-Pinilla, D. Sarrio, G. Moreno-Bueno, Y. Rodriguez-Gil, M. Martinez, L. Hernandez, D. Hardisson, J.S. Reis-Filho, J. Palacios, Sox2: a possible driver of the basal-like phenotype in sporadic breast cancer. Mod. Pathol. **20**, 474–481 (2007)
38. R.M.R. Gangemi, F. Griffero, D. Marubbi, M. Perera, M.C. Capra, P. Malatesta, G.L. Ravetti, G.L. Zona, A. Daga, G. Corte, SOX2 silencing in glioblastoma tumor-initiating cells causes stop of proliferation and loss of tumorigenicity. Stem Cells **27**, 40–48 (2009)
39. H. Ikushima, T. Todo, Y. Ino, M. Takahashi, K. Miyazawa, K. Miyazono, Autocrine TGF-beta signaling maintains tumorigenicity of glioma-initiating cells through Sry-related HMG-box factors. Cell Stem Cell **5**, 504–514 (2009)
40. A.C. Laga, C.-Y. Lai, Q. Zhan, S.J. Huang, E.F. Velazquez, Q. Yang, M.-Y. Hsu, G.F. Murphy, Expression of The Embryonic Stem Cell Transcription Factor SOX2 in Human Skin. Am. J. Pathol. **176**, 903–913 (2010)
41. V. Carina, G. Zito, G. Pizzolanti, P. Richiusa, A. Criscimanna, V. Rodolico, L. Tomasello, M. Pitrone, W. Arancio, C. Giordano, Multiple pluripotent stem cell markers in human anaplastic

thyroid cancer: the putative upstream role of SOX2. Thyroid **23**, 829–837 (2013)
42. R. Jauch, I. Aksoy, A.P. Hutchins, C.K.L. Ng, X.F. Tian, J. Chen, P. Palasingam, P. Robson, L.W. Stanton, P.R. Kolatkar, Conversion of Sox17 into a pluripotency reprogramming factor by reengineering its association with Oct4 on DNA. Stem Cells **29**, 940–951 (2011)
43. I. Aksoy, R. Jauch, J. Chen, M. Dyla, U. Divakar, G.K. Bogu, R. Teo, C. Keow, L. Ng, W. Herath, S. Lili, P. Hutchins, P. Robson, P.R. Kolatkar, L.W. Stanton, Oct4 switches partnering from Sox2 to Sox17 to reinterpret the enhancer code and specify endoderm. EMBO J. **32**, 938–953 (2013)
44. Y. Chao, Q. Wu, C. Shepard, A. Wells, Hepatocyte induced re-expression of E-cadherin in breast and prostate cancer cells increases chemoresistance. Clin. Exp. Metastasis **29**, 39–50 (2012)
45. Y. Chao, Q. Wu, M. Acquafondata, R. Dhir, A. Wells, Partial mesenchymal to epithelial reverting transition in breast and prostate cancer metastases. Cancer Microenviron. **5**, 19–28 (2012)
46. T. Sasaki, J. Koivunen, A. Ogino, M. Yanagita, S. Nikiforow, W. Zheng, C. Lathan, J.P. Marcoux, J. Du, K. Okuda, M. Capelletti, T. Shimamura, D. Ercan, M. Stumpfova, Y. Xiao, S. Weremowicz, M. Butaney, S. Heon, K. Wilner, J.G. Christensen, M.J. Eck, K.-K. Wong, N. Lindeman, N.S. Gray, S.J. Rodig, P. aJänne, A novel ALK secondary mutation and EGFR signaling cause resistance to ALK kinase inhibitors. Cancer Res. **71**, 6051–6060 (2011)
47. R. Katayama, A.T. Shaw, T.M. Khan, M. Mino-kenudson, B.J. Solomon, B. Halmos, N.A. Jessop, J.C. Wain, A. Tien, C. Benes, L. Drew, J.C. Saeh, K. Crosby, V. Lecia, A.J. Iafrate, J.A. Engelman, Mechanisms of acquired crizotinib resistance in ALK-rearranged lung cancers. Sci. Transl. Med. **4**, 1–25 (2012)
48. J. Tanizaki, I. Okamoto, T. Okabe, K. Sakai, K. Tanaka, H. Hayashi, H. Kaneda, K. Takezawa, K. Kuwata, H. Yamaguchi, E. Hatashita, K. Nishio, K. Nakagawa, Activation of HER family signaling as a mechanism of acquired resistance to ALK inhibitors in EML4-ALK-positive non-small cell lung cancer. Clin. Cancer Res. **18**, 6219–6226 (2012)
49. A. Wunderlich, S. Roth, A. Ramaswamy, B.H. Greene, I.C. Brende, U. Hinterseher, D.K. Bartsch, S. Hoffmann, Combined inhibition of cellular pathways as a future therapeutic option in fatal anaplastic thyroid cancer. Endocrine **42**, 637–646 (2012)